JOURNAL OF GEOPHYSICAL RESEARCH, VOL. 103, NO. A4, PAGES 6663–6674, APRIL 1, 1998

Magnetic field rotation at the dayside magnetopause: AMPTE/IRM observations

J. De Keyser and M. Roth

Belgian Institute for Space Aeronomy, Brussels

Abstract. Given the large-scale magnetosheath flow pattern around the magnetosphere, the tangential discontinuity magnetopause model of De Keyser and Roth predicts, for a prescribed magnetic field rotation angle and rotation sense, where equilibrium is possible on the dayside magnetopause surface and where it is not. In this paper we verify these predictions using 5 s time resolution magnetic field and plasma observations of the low-latitude dayside magnetospheric boundary acquired by the Active Magnetospheric Particle Tracer Explorers/Ion Release Module satellite. The model is confirmed by (1) the dominant presence of large positive magnetic field rotations among the dawnside crossings north of the equator, (2) the observation of positive and negative rotations near the stagnation point and at the duskside, and (3) the rare occurrence and questionable tangential discontinuity nature of low magnetic shear dawnside crossings. The absence of tangential discontinuity equilibrium in dawnside low shear crossings is consistent with the observation of increased dawnside low-latitude boundary layer thickness for northward magnetosheath field reported in the literature.

1. Introduction

The magnetospheric boundary interfaces the shocked solar wind in the dayside magnetosheath with the plasma inside the magnetospheric cavity. The magnetospheric boundary consists of the magnetopause (MP), the layer that carries the current responsible for the rotation of the magnetic field from its magnetosheath direction to the northward dipole field, and the low-latitude boundary layer (LLBL) adjacent to the earthward edge of the magnetopause, which contains a mixture of magnetosheath and magnetospheric plasma [*Eastman et al.*, 1976]. Average profiles of magnetic field, plasma density, and temperature variations throughout the MP/LLBL region have been obtained by *Paschmann et al.* [1993] and *Phan and Paschmann* [1996] from Active Magnetospheric Particle Tracer Explorers/Ion Release Module (AMPTE/IRM) observations. Magnetic field and plasma properties progressively change from their magnetosheath to magnetospheric values. The magnetospheric plasma is 5–10 times less dense and 5 times hotter than the magnetosheath plasma [e.g., *Paschmann et al.*, 1993; *Phan and Paschmann*, 1996]. The magnetic field, while rotating fast inside the magnetopause, continues to rotate slowly up to the LLBL inner edge.

It is not always obvious to identify the MP and LLBL unambiguously in satellite observations as the magnetospheric boundary is constantly in motion in response to the variable solar wind pressure. This motion may lead to multiple encounters of a satellite with the MP/LLBL region during a single pass. Translating the observed time series into spatial profiles would require a deconvolution with the magnetopause velocity component normal to the magnetopause surface. This velocity is generally not known with sufficient accuracy and time resolution [*Phan and Paschmann*, 1996].

Theoretical descriptions of the magnetospheric boundary often consider the magnetopause to be a tangential discontinuity (TD) and try to establish under what circumstances such an impermeable boundary can exist. The present paper focuses on a recent kinetic model of the TD magnetopause by *De Keyser and Roth* [1997a, b, this issue] (henceforth called the "DKR model") that emphasizes the importance of the plasma velocity change across the layer. This velocity change varies from zero at the stagnation point up to nearly the undisturbed solar wind speed at the flanks. It gives rise to a convection electric field that, apart from thermoelectric contributions due to temperature gradients, determines the structure of the transition layer [see also *Sestero*, 1966; *Cargill and Eastman*, 1991; *Kuznetsova et al.*, 1994]. The DKR model shows that TD equilibrium is possible only for certain combinations of magnetic field and shear flow orientations. Taking the shear flow across the magnetospheric boundary to be essentially the magnetosheath flow, the DKR model is able to predict which regions of the dayside magnetopause can be in TD equilibrium for a prescribed magnetosheath field orientation, that is, for a prescribed magnetic field rotation sense and rotation angle.

Of particular importance for the magnetic field sense-of-rotation issue is the rotational discontinuity (RD) model of *Su and Sonnerup* [1968]. Using first-order orbit theory for wide RDs, they predict a clockwise rotation of the tangential magnetic field vector from its magnetospheric to its mag-

Paper number 97JA03711.
0148-0227/98/97JA-03711$09.00

netosheath direction in the northern hemisphere and counterclockwise rotation in the southern hemisphere: the magnetic field rotation has the electron polarization sense of a large-amplitude Alfvén wave. While this model is in agreement with Explorer 12 observations [*Sonnerup and Cahill*, 1968], it was found to be incompatible with ISEE 1 and 2 data [*Berchem and Russell*, 1982].

The purpose of this paper is to verify the predictions of the DKR model regarding the magnetic field sense-of-rotation issue by confronting it with AMPTE/IRM observations of the dayside magnetopause. In the first part of this paper we check the predicted relationship between the magnetic field and the velocity jump across a TD, that is, we check whether the observed magnetic field/velocity jump configurations satisfy the equilibrium conditions outlined by *De Keyser and Roth* [1997a, this issue]. The second part of the paper deals with the sense of the magnetic field rotation. The merit of this paper lies in the experimental confirmation of these predictions, thereby contributing to the sense-of-rotation debate for the TD case and improving our understanding of the physical mechanisms that govern the structure of the dayside magnetopause.

2. AMPTE/IRM Observations

AMPTE/IRM was one of three satellites in the Active Magnetospheric Particle Tracer Explorers program. It was launched in August 1984. The data used in this study are taken from the first months of the AMPTE/IRM mission, from September to December 1984. The orbit originally had its apogee at 18.7 R_E in the sunward direction (1300 magnetic local time (MLT)). With an inclination of 28.5° and a 43.8 hour orbital period it crossed the low-latitude dayside MP about once per day (not all of these crossings occurred while the satellite was tracked). Due to the Earth's orbital motion the apogee direction relative to the noon meridian shifted about 30° per month (0200 MLT/month) dawnward. By the end of 1984 the elliptical orbit started to point tailward and the dayside magnetopause was no longer encountered. The data used in this study were recorded by the three-dimensional plasma electrostatic analyzer instrument [*Paschmann et al.*, 1985] and the fluxgate magnetometer [*Lühr et al.*, 1985]. From the plasma instrument we obtained ion and electron number densities and temperatures and the plasma bulk velocity. We use the observed ion density as indicator of the plasma density.

AMPTE/IRM 5-s resolution magnetic field and plasma data were visually scanned. For each passage through the MP/LLBL layer we identify one or, in the case of multiple crossings, several MP crossings, based on inspection of magnetic field and plasma density, temperature, and velocity profiles. As there is nearly always a pronounced plasma density and/or temperature difference across the transition, even in the case of low magnetic shear [e.g., *Paschmann et al.*, 1993], no crossing remains unnoticed. We try to define the uniform plasma and field states on either side of the transition. The magnetic field on the magnetosheath side typically fluctuates, so that the magnetic field rotation angle is not always well determined. This may be particularly troublesome for low magnetic shear crossings, where the distinction between the magnetopause and solar wind directional discontinuities embedded in the adjacent magnetosheath is less obvious [*Paschmann et al.*, 1993]. The earthward state may be either inside the LLBL (when it is sufficiently broad and the magnetic field and plasma properties are fairly constant) or in the magnetosphere proper (for instance, when the LLBL is thin or absent). This ambiguity in defining the earthward state is not important for our analysis as the magnetic field in the LLBL and the magnetosphere do not differ much, and as the plasma velocity in the magnetosphere and in the LLBL sufficiently earthward of the magnetopause are both small compared to the magnetosheath flow. Whenever the superscript "msph" is used below, this is meant to indicate the magnetospheric side of the magnetopause current layer; this can be either the magnetosphere proper or the earthward portion of the LLBL. For each transition we determine the minimum variance frame (MVF). Special attention was paid to the plasma velocity component perpendicular to the (locally planar) MP surface. This normal velocity reveals the magnetopause motion as the magnetosphere expands or is compressed in response to variations in solar wind pressure. Inspection of the normal velocity helps the interpretation of multiple crossings by showing that the different magnetopause encounters observed during the same pass are indeed due to MP motion and by indicating which of the MP encounters are only partial. We discarded crossings recorded when major interplanetary magnetic field disturbances were present. We have analyzed 58 transitions from 45 distinct passes in detail (among which four transitions from four distinct passes for which no plasma data were available).

Each transition is first transformed into its proper MVF, with x, y, and z axes corresponding to the minimum, intermediate, and maximum variance directions. The x axis then represents the magnetopause normal, while the yz plane coincides with the magnetopause surface which is considered to be locally planar. We then make sure that the x axis points outward; if not, a 180° rotation around the z axis is applied. Subsequently, a rotation around the x axis is carried out to align y with the bisectrix of the magnetospheric and magnetosheath magnetic field vectors $\boldsymbol{B}^{\mathrm{msph}}$ and $\boldsymbol{B}^{\mathrm{msh}}$, such that $B_y^{\mathrm{msph}} \geq 0$ and $B_y^{\mathrm{msh}} \geq 0$. The resulting reference frame is the one used in the DKR model (Figure 1). For each transition we determine (1) the magnitude and the sense of the magnetic field rotation angle θ_B; (2) the magnetic field asymmetry factor $\kappa_B = 1 - B^{\mathrm{msh}}/B^{\mathrm{msph}}$ as defined by *Kuznetsova and Roth* [1995]; (3) the average normal magnetic field component $\bar{B}_x$; (4) the transition thickness $2D = \int_{t_{\mathrm{begin}}}^{t_{\mathrm{end}}} V_x dt = \bar{V}_x(t_{\mathrm{end}} - t_{\mathrm{begin}})$, where V_x is the normal plasma bulk velocity. The crossing time interval $[t_{\mathrm{begin}}, t_{\mathrm{end}}]$ is determined by visual inspection of the magnetic field profile. This thickness estimate is very crude because t_{begin} and t_{end} are not always unambiguously defined and because of the uncertainty on V_x (slight misalignment of the MVF may significantly affect its value). Furthermore, this estimate is only valid for TDs and for RDs where the plasma motion through the discontinuity (Alfvén

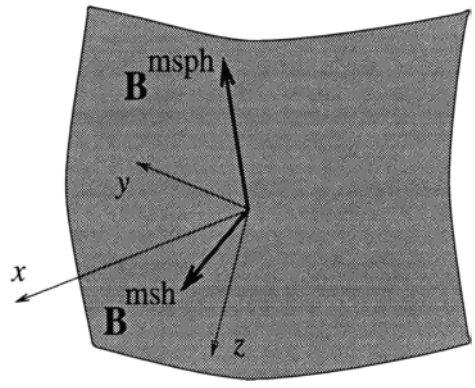

Figure 1. The reference frame used in the DKR model [*De Keyser and Roth*, 1997a] is a rotated boundary normal coordinate system: x is the outward-pointing magnetopause normal, y is the inner bisectrix of the magnetosheath and magnetospheric magnetic fields $\boldsymbol{B}^{\mathrm{msh}}$ and $\boldsymbol{B}^{\mathrm{msph}}$ (i.e., $B_y^{\mathrm{msh}} \geq 0$ and $B_y^{\mathrm{msph}} \geq 0$), and z completes the right-handed orthogonal set. The yz plane coincides with the (locally planar) magnetopause.

speed based on the normal magnetic field component) is significantly slower than the speed of the spacecraft relative to the discontinuity. We also determine (5) the proton thermal velocity $V_{th}^{\mathrm{msh}+} = \sqrt{2kT^{\mathrm{msh}+}/m^+}$ and gyroradius $\rho^{\mathrm{msh}+} = m^+V_{th}^{\mathrm{msh}+}/eB^{\mathrm{msh}}$ in the magnetosheath adjacent to the magnetopause; these are computed from B^{msh}, the proton mass m^+, and the magnetosheath temperature $T^{\mathrm{msh}+}$. We will use $\rho^{\mathrm{msh}+}$ and $V_{th}^{\mathrm{msh}+}$ as reference length and speed. We further determine (6) the bulk velocity jump $\boldsymbol{V}_r = \boldsymbol{V}^{\mathrm{msh}} - \boldsymbol{V}^{\mathrm{msph}}$ across the magnetopause; (7) the magnetosheath and magnetospheric magnetic pressure $P_{mag} = B^2/2\mu_0$; (8) the magnetosheath and magnetospheric thermal pressure, estimated by $P_{th} = kN^+(T^+ + T^-)$; the contribution of heavy ions is not accounted for, possibly leading to an error of up to 20%, as indicated by detailed pressure calculations including He^{++}, He^+ and O^+ [*Eastman et al.*, 1996]; (9) the magnetosheath and magnetospheric total plasma pressure $P = P_{th} + P_{mag}$; (10) the magnetosheath and magnetospheric plasma beta $\beta = P_{th}/P_{mag}$.

Individual crossings observed during the same pass are not independent. For instance, the sense of magnetic field rotation usually is the same for all crossings in a given pass, as expected for a MP that is moving back and forth. We therefore have selected the most representative transition from each pass. This guarantees the statistical independence of the data points [*Sonnerup and Cahill*, 1968; *Berchem and Russell*, 1982]. Whenever multiple transitions were analyzed for the same pass, we checked whether similar magnetic field rotation angle, velocity jump, and plasma parameters were found for all of them. This reassured us that no severe errors were made, in particular in establishing the MVF (which may be ill defined in the case of essentially unidirectional magnetic field variations, a situation typical for, but not limited to, low magnetic shear crossings). Table 1 lists the main properties of the crossings considered in this study.

We have checked the plasma pressure balance condition $P^{\mathrm{msh}}/P^{\mathrm{msph}} = 1$ in order to verify the quality of the data set. Figure 2 presents the histogram of $P^{\mathrm{msh}}/P^{\mathrm{msph}}$. The bulk of the distribution lies between 0.7 and 1.1, with a mean of 0.97. Bearing in mind the uncertainties on densities and temperatures, the data set can be assumed to be representative of equilibrium or slow time evolution. It should be noted that isotropic temperatures have been used in evaluating the pressure balance, while only the perpendicular temperature actually matters in a one-dimensional configuration.

Figure 3 displays the distribution of the average normal magnetic field component $\bar{B}_x$ relative to the magnetospheric field strength B^{msph}. This plot indicates that the data set includes TDs and small normal field RDs, with only a few exceptions. We therefore expect the DKR model (for TDs) to be applicable.

3. Magnetic Field/Flow Shear Configurations

The original DKR model [*De Keyser and Roth*, 1997a, b] describes symmetric transitions ($\kappa_B = 0$) between identical plasmas with $N^{\mathrm{msph}} = N^{\mathrm{msh}}$ and $T^{\mathrm{msph}-} = T^{\mathrm{msph}+} = T^{\mathrm{msh}-} = T^{\mathrm{msh}+}$. This model was later extended in order to relax these constraints on plasma densities and temperatures [*De Keyser and Roth*, this issue]. The model shows that, for a given magnetic field configuration, only a limited set of velocity jump vectors $\boldsymbol{V}_r$ lead to TD equilibrium. The purpose of this section is to outline the theoretical $\boldsymbol{V}_r$ domain for the observed plasma parameters and to confront it with the $\boldsymbol{V}_r$ diagram derived from the AMPTE/IRM observations.

3.1. Theoretical Velocity Jump Diagram

The DKR model describes the non-Maxwellian velocity distribution functions (VDFs) in terms of a so-called transition length parameter $\mathcal{L}$. This parameter is the characteristic length scale of variations in the moments of the VDFs. One expects the proton transition length $\mathcal{L}_+$ to be larger than the electron transition length $\mathcal{L}_-$ because of the larger proton gyroradius [*De Keyser and Roth*, 1997a]. Both, however, should not differ too much in order to avoid charge separation effects that would lead to strong local electric fields, a situation believed to be unstable.

Only protons and electrons are considered in the DKR model. In addition to the magnetospheric and magnetosheath particles, the model also incorporates inner populations that are confined to the magnetopause current layer, also called "trapped" populations [*Lee and Kan*, 1979]. Inner proton and electron populations have a mean drift velocity V_d in opposite directions in the TD plane, more or less perpendicular to the magnetic field change. The thickness of the drift current layer is characterized by a length scale $\mathcal{L}_d$, which is related to the drift speed by [*Harris*, 1962]

$$V_d = \frac{2kT}{\mathcal{L}_d eB} = \frac{\rho^+}{\mathcal{L}_d} V_{th}^+.$$

Since the DKR model relates the transition thickness to the characteristic lengths, it is in principle possible to use the AMPTE/IRM thickness measurements in order to constrain the characteristic length values. In practice this is not obvious because the effects of $\mathcal{L}_+$, $\mathcal{L}_-$, and $\mathcal{L}_d$ are hard to sep-

Table 1. AMPTE/IRM Magnetopause Crossings

Date	Inbound (I) or Outbound (O)	Longitude, deg. (GSM)	Latitude, deg. (GSM)	θ_B, deg.	V_τ/V_{th}^+	θ_τ, deg.
Sept. 1, 1984	O	5	2	-131	0.14	6
Sept. 2, 1984	I	46	-19	-151	0.86	-6
Sept. 4, 1984	I	58	-27	-73	1.02	-28
Sept. 4, 1984	O	1	4	59	0.45	-127
Sept. 6, 1984	O	-1	4	124	0.21	-110
Sept. 8, 1984	O	-4	7	108	0.30	-132
Sept. 10, 1984	O	-1	5	86	0.41	-123
Sept. 11, 1984	I	39	-9	52	0.79	-126
Sept. 12, 1984	O	-3	6	-102	0.14	103
Sept. 13, 1984	I	39	-14	78	0.75	-148
Sept. 14, 1984	O	-7	7	98	0.27	-139
Sept. 15, 1984	I	33	-19	136	1.03	-170
Sept. 16, 1984	O	-8	6	164	0.23	-64
Sept. 17, 1984	O	-9	5	-106	0.06	-35
Sept. 19, 1984	O	-15	11	-86	0.12	62
Sept. 21, 1984	I	31	-10	-111	0.81	-38
Sept. 21, 1984	O	-13	12	-64	0.37	88
Sept. 23, 1984	I	35	-10	-133	0.81	-40
Sept. 23, 1984	O	-20	17	-134	0.12	105
Sept. 24, 1984	I	32	-9	153	0.63	-176
Sept. 25, 1984	O	-15	12	-137	0.17	135
Sept. 26, 1984	I	23	-13	-176	0.27	-111
Sept. 28, 1984	I	24	-17	-108	0.54	-52
Oct. 6, 1984	O	-24	18	-76	–	–
Oct. 8, 1984	O	-27	14	156	0.51	-38
Oct. 9, 1984	I	16	-11	-153	0.43	-53
Oct. 11, 1984	I	15	-13	84	0.36	160
Oct. 15, 1984	O	-33	22	150	0.43	-37
Oct. 19, 1984	O	-39	19	-142	–	–
Oct. 24, 1984	I	6	-7	-170	0.22	-26
Oct. 28, 1984	O	-42	23	95	0.77	-4
Oct. 30, 1984	O	-44	24	75	0.64	19
Nov. 1, 1984	O	-53	15	-102	–	–
Nov. 4, 1984	I	-3	-2	44	–	–
Nov. 10, 1984	O	-57	26	-3	0.96	64
Nov. 12, 1984	O	-58	21	174	0.87	-25
Nov. 21, 1984	O	-71	27	112	1.26	17
Nov. 23, 1984	O	-66	22	166	1.23	-24
Nov. 25, 1984	O	-71	13	139	1.20	25
Nov. 28, 1984	I	-28	7	113	0.59	5
Dec. 4, 1984	O	-79	19	128	0.99	-7
Dec. 6, 1984	O	-77	16	172	1.32	-32
Dec. 8, 1984	O	-83	0	177	1.02	-76
Dec. 9, 1984	I	-39	7	59	0.47	30
Dec. 11, 1984	I	-36	4	-55	0.61	93

arate. Moreover, the thickness estimates have a large error margin. We found ion transition length $\mathcal{L}_+$ estimates varying between 1 and 5 $\rho^{\mathrm{msh}+}$, and $\mathcal{L}_-$ values up to 3 $\rho^{\mathrm{msh}+}$. Also $\mathcal{L}_d$ appears to be of the order of a few ion gyroradii.

Typical plasma parameter values for the AMPTE/IRM data set are shown in the histograms of Figures 4–6. The magnetosheath beta β^{msh} most often is between 0.5 and 4 (Figure 4), reflecting the variability in solar wind conditions over the period of observation (several months). The magnetospheric plasma beta $\beta^{\mathrm{msph}} \approx 0.2$ does not vary much (Figure 5). The change in magnetic field magnitude across the magnetopause is quantified by the magnetic field asymmetry factor κ_B defined earlier. Figure 6 shows that symmetric transitions ($\kappa_B = 0$) are relatively rare. A moderate asymmetry with $B^{\mathrm{msh}}/B^{\mathrm{msph}} = 3/5$ is typical. Note that, even for symmetric transitions, plasma densities and temperatures on either side usually are different. The pressure balance condition shows that β^{msh}, β^{msph}, and κ_B are not independent. Indeed, from

$$
\begin{aligned}
P_{mag}^{\mathrm{msph}} + P_{th}^{\mathrm{msph}} &= P_{mag}^{\mathrm{msh}} + P_{th}^{\mathrm{msh}}, \\
\frac{P_{mag}^{\mathrm{msph}}}{P_{mag}^{\mathrm{msh}}} &= \frac{1+\beta^{\mathrm{msh}}}{1+\beta^{\mathrm{msph}}}, \\
\frac{1}{(1-\kappa_B)^2} &\approx 1+\beta^{\mathrm{msh}},
\end{aligned}
$$

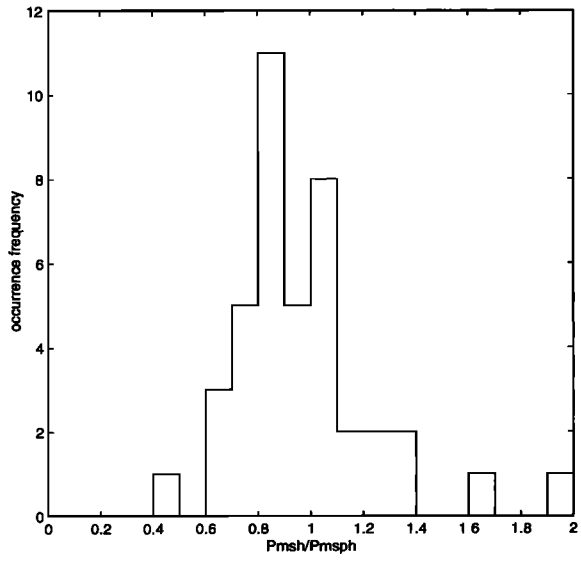

Figure 2. Histogram of the magnetosheath–magnetosphere total plasma pressure ratio $P^{\mathrm{msh}}/P^{\mathrm{msph}}$. The median of the distribution lies slightly below 1. The spreading of the distribution is consistent with the uncertainty in plasma properties. Except for a few individual cases, the transitions in the data set can be assumed to be in a state of pressure balance.

where the last step is based on the observation that typically $\beta^{\mathrm{msph}} < 1$, it is found that

$$\kappa_B \approx 1 - \frac{1}{\sqrt{1+\beta^{\mathrm{msh}}}}.$$

The experimental verification of this relation is shown in Figure 7. The agreement is pretty good, again confirming pressure balance. It shows that, at least for this particular data set, either β^{msh} or κ_B can be used as the single parameter characterizing the magnetopause environment.

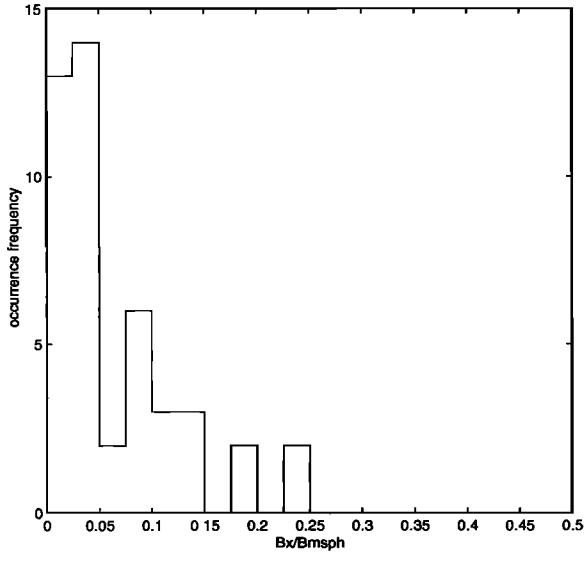

Figure 3. Histogram of the average normal magnetic field component relative to the magnetospheric field strength. Except for a few individual cases, the data set contains only TDs and small normal field RDs.

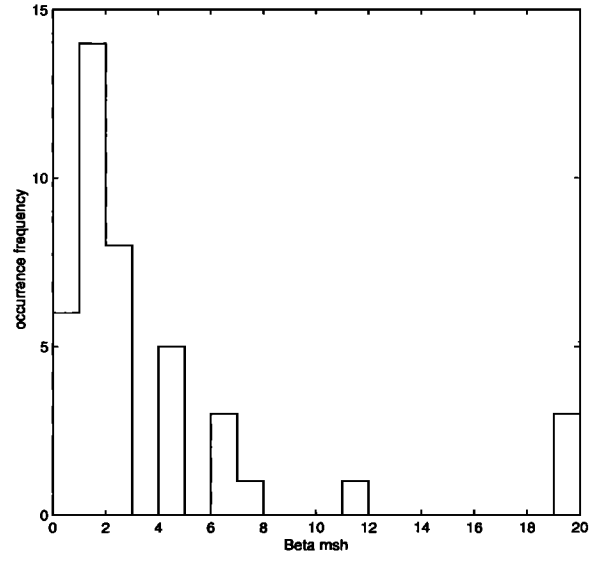

Figure 4. Histogram of magnetosheath plasma beta, showing the range of magnetosheath conditions present in the AMPTE/IRM data set.

Given the plasma parameters and the transition lengths, the velocity jump vector domain for which the DKR model admits equilibrium can be outlined by numerically computing the structure of the transition for different velocity jumps, and checking whether a solution exists that meets the boundary conditions (uniform magnetic fields on either side of the transition, rotated over a specified angle θ_B). Figure 8 (taken from *De Keyser and Roth* [this issue]) sketches the velocity jump domain for the case of symmetric and asymmetric transitions. The plasma parameters used to construct these diagrams agree with the typical values found in the AMPTE/IRM observations. These diagrams are obtained by superposition of individual diagrams computed for a range

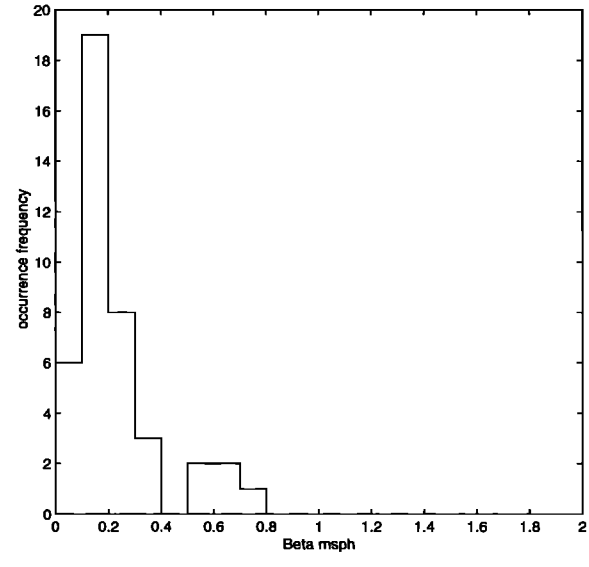

Figure 5. Histogram of magnetospheric plasma beta. The typical value is $\beta^{\mathrm{msph}} \approx 0.2$.

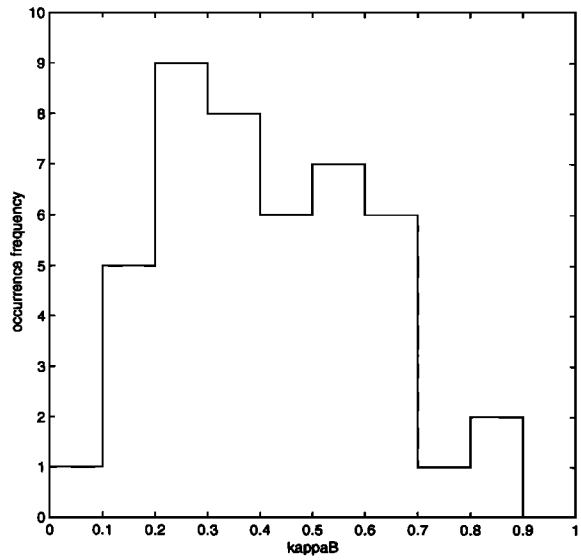

Figure 6. Histogram of the magnetic field asymmetry κ_B. Symmetric transitions are relatively rare; a magnetospheric to magnetosheath magnetic field ratio of 5 to 3 is typical.

of transition length values $\mathcal{L}_+$ and $\mathcal{L}_-$, drift current layer thickness scale $\mathcal{L}_d$, and plasma densities and temperatures. While Figure 8a is symmetric with respect to the V_{rz} axis (and is the same for positive and negative magnetic field rotation angles θ_B), Figure 8b is not: the skewness increases with the rotation angle and depends on the sense of rotation (the deformation is due to thermoelectric effects at the interface between plasmas with different temperature). The dashed half circles correspond to $V_r/V_{th}^+ \approx 1.4$, the maximum relative velocity at the dayside magnetopause inferred from dawnside AMPTE/IRM crossings; the precise form of the existence domain outside this circle therefore is of no interest here. Figure 8 leads to the conclusion that, for large shear flow ($V_r/V_{th}^+ \gtrsim 0.5$), not just any shear flow direction is admitted. The existence domain is largest for $V_{rz} < 0$, but some fraction of the upper quadrants is covered as well, especially for asymmetric transitions.

3.2. Observed Velocity Jump Diagram

Figure 9 is a plot in the yz frame (see Figure 1) of the vector $\boldsymbol{V}_r/V_{th}^{\mathrm{msh}+}$ for each magnetopause crossing. The orientation of the y axis depends on the magnetic field rotation angle θ_B and must be recomputed for each transition. Low magnetic shear crossings ($|\theta_B| \leq 60°$) are indicated by a circle, large positive magnetic field rotations ($\theta_B > 60°$) by a plus, and large negative rotations ($\theta_B < -60°$) by a minus.

The AMPTE/IRM orbit does not sample the dayside MP at all latitudes and longitudes. While the GSM latitude coverage is rather limited ($-30°$ to $+30°$), almost the entire range in GSM longitude is covered (longitude $-90°$ to $+60°$, that is, 0600 to 1600 MLT). The data set therefore explores the full range of $V_r/V_{th}^{\mathrm{msh}+}$ magnitudes encountered in the dayside magnetosheath, with large velocity jumps $V_r/V_{th}^{\mathrm{msh}+} \approx 1.4$ at the dawnside and the duskside, and small jumps close to the stagnation point. Since the data set covers all magnetic field rotation angles, all possible orientations of $\boldsymbol{V}_r/V_{th}^{\mathrm{msh}+}$ in the yz frame are a priori possible. The large velocity jump cases in the data set correspond to low-latitude dawnside and duskside crossings, where the magnetosheath velocity is responsible for the major part of the jump. The data set therefore comprises only large velocity jumps where $\boldsymbol{V}_r$ is more or less perpendicular to $\boldsymbol{B}^{\mathrm{msph}}$.

The distribution of the data points in the velocity jump diagram of Figure 9 is clearly not uniform. A first observation is, of course, the limitation $V_r/V_{th}^{\mathrm{msh}+} < 1.4$, which reflects the magnetosheath conditions at the dawnside and the duskside. A second observation is that the upper two quadrants of the diagram are less populated than the lower quadrants. We have estimated the statistical significance of this uneven distribution by testing the hypothesis that there is no directional dependence, that is, that θ_r (the polar angle of $\boldsymbol{V}_r$) is distributed uniformly over $[-180°, +180°]$. Breaking up the data set in eight 45° wide classes (the largest number of classes that still has sufficient observations per class), Pearson's χ^2 test leads to a rejection of this hypothesis at the 97% confidence level. A third observation is that crossings with a large velocity shear component along the $+z$ axis are absent (except for one or two low shear crossings), while smaller velocity jumps can have any orientation.

Figure 9 is a mix of magnetopause transitions in all sorts of regimes (different transition lengths, plasma properties, and so on). The superposition of existence domains sketched in Figure 8, computed for typical values of the transitions lengths, plasma beta, proton/electron and magnetosphere/magnetosheath temperature ratios and for various magnetic field rotation angles, was intended to mimic this. The distribution of points corresponding to large positive magnetic field rotation in Figure 9 (pluses) is consistent with Figure 8.

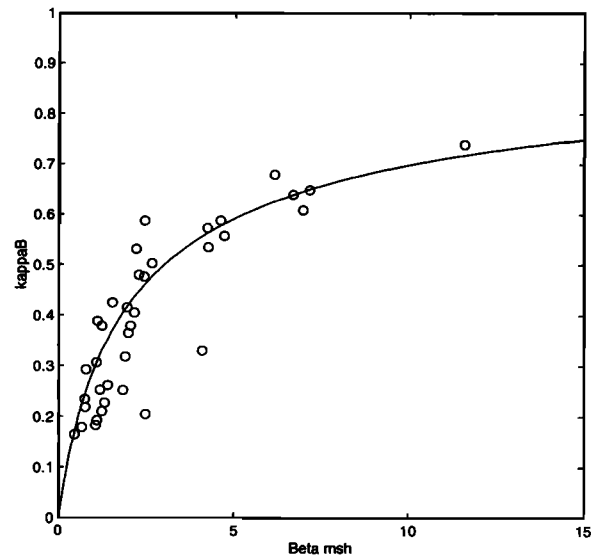

Figure 7. Magnetic field asymmetry κ_B as a function of β^{msh}. The circles indicate the AMPTE/IRM observations; the solid line corresponds to the relation discussed in the text.

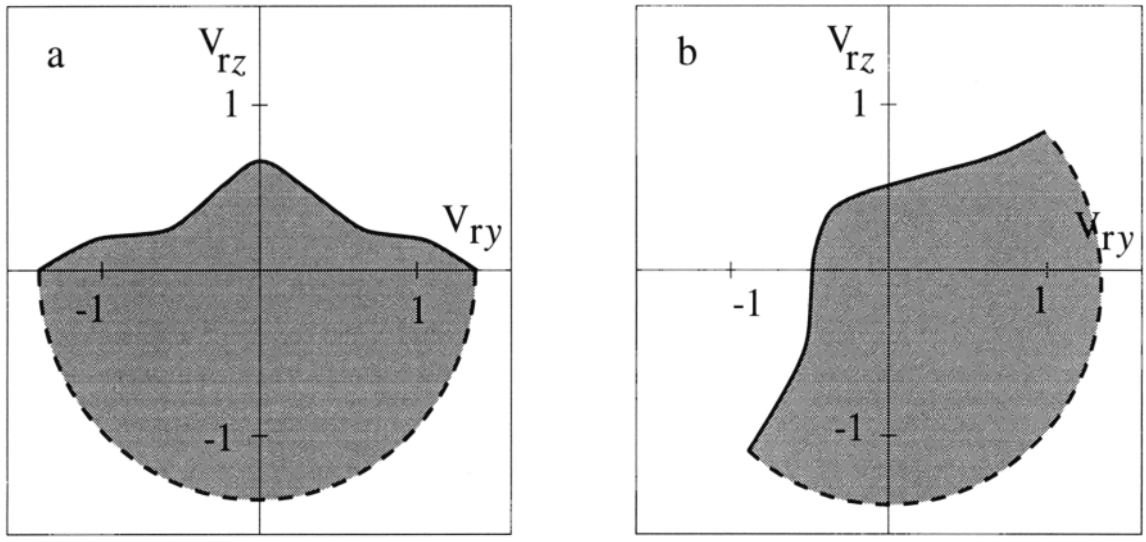

Figure 8. Velocity jump vector domains for (a) symmetric and (b) asymmetric transitions. Figure 8a sketches the domain obtained by superposition of existence domains for typical transition lengths and plasma parameters, all for ±90° rotation angle; for other rotation angles one finds essentially the same type of domain. The dashed half circle corresponds to the maximum velocity jump magnitude encountered at the dayside magnetopause; the shape of the domain outside this circle is of no interest here. Figure 8b is a similar superposition for asymmetric plasma conditions, corresponding to a +90° rotation; in the asymmetric case the shape of the domain varies with the rotation angle. (Adapted from *De Keyser and Roth* [this issue]).

There are some points in the upper quadrants near the $+y$ axis, as would be expected for asymmetric transitions with positive rotation angle (like in Figure 8b). The distribution of points corresponding to large negative magnetic field rotation is also consistent with the theoretical domains of Figures 8; the lack of data points near the $-y$ axis corresponds to an absence of large negative rotations among the dawnside AMPTE/IRM crossings (which all occurred at northern latitude). The agreement with the theoretical existence domain demonstrates that the high magnetic shear crossings in the data set (a mix of TDs and RDs) do indeed obey the existence conditions implied by the DKR model. The situation seems more complicated for low magnetic shear. A few low-shear crossings were observed near the dawnside, leading to points with large positive V_{rz}/V_{th}^{+}. In particular, the November 10, 1984 crossing (with $V_{rz}/V_{th}^{+} \approx 0.9$) seems to contradict the DKR model, which considers low-shear dawnside equilibria improbable. A detailed analysis of this case would be required to check whether there really is a contradiction when the actually observed plasma properties are considered; information on the velocity distribution functions could help to constrain the values of the transition lengths. Moreover, detailed studies of this particular crossing by *Hall et al.* [1990] and similar ones by *Paschmann et al.* [1990] suggest that the TD nature of these low-shear crossings is questionable, since at least part of the LLBL appears to be on open field lines. Other observations reveal an increased LLBL width in the low magnetic shear dawnside magnetospheric boundary [*Mitchell et al.*, 1987; *Sauvaud et al.*, 1997], which similarly points to a loss of TD equilibrium.

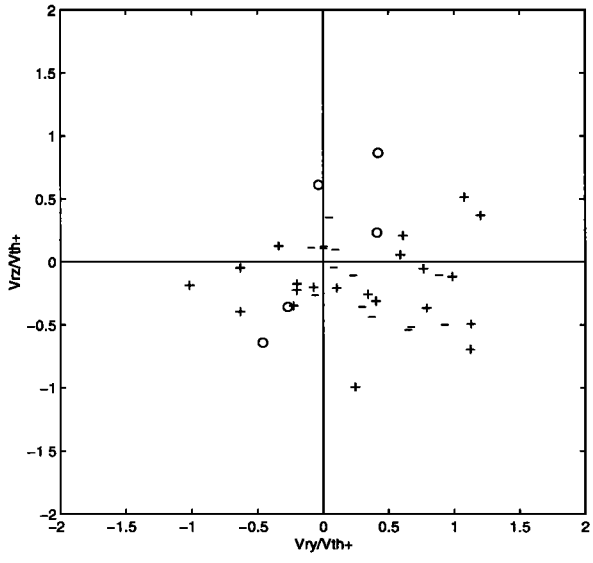

Figure 9. Plot in the yz frame (see Figure 1) of the vector $V_r/V_{th}^{\mathrm{msh}+}$ for each AMPTE/IRM magnetopause crossing. Low magnetic shear crossings ($|\theta_B| < 60°$) are indicated by a circle, large positive magnetic field rotations ($\theta_B > 60°$) are indicated by a plus, and large negative rotations ($\theta_B < -60°$) are indicated by a minus.

We have made a similar comparison for a TD subset of the AMPTE/IRM crossings for which $B_x/B^{\mathrm{msph}} < 0.05$. The same general agreement was found. It is interesting to note that the B_x value does not seem to be correlated to the magnitude of the velocity shear across the layer.

It can be concluded that the theoretical velocity jump domain is qualitatively consistent with the observations. This

evidence supports the argument that the electric field determines the structure of the magnetopause. This electric field is mainly determined by the orientation of the shear flow with respect to the magnetic field. This is especially true for strong flow gradients, although thermoelectric contributions also may affect the electric field. The different response of ions and electrons to this field explains why the behaviour of the layer is sensitive to the shear flow orientation.

4. Magnetic Field Rotation Sense

The previous section led to a confirmation of the DKR model regarding the existence of TD equilibrium. *De Keyser and Roth* [this issue] have shown that these existence conditions can be used to identify regions on the dayside magnetopause where equilibrium is admitted for a given magnetic field rotation. In this section we compare this theory with the AMPTE/IRM observations.

4.1. Theoretical Predictions

Knowledge of the magnetosheath flow is a prerequisite if the DKR model is to be used to obtain a general picture of the existence of TD equilibrium at the dayside magnetopause. We assume that the magnetosheath plasma flows radially away from the stagnation point. The position of the stagnation point is taken to be in the solar wind inflow direction as measured by AMPTE/IRM right in front of the bow shock. Its mean location was found to be in the GSM equatorial plane, about 5° dawnward of the subsolar point, with a standard deviation of 3° in both longitude and latitude. This is only an approximation as the inflow direction can change between the time of passage through the bow shock and the magnetopause. It is also known that the stagnation point in the magnetosheath flow may be shifted some distance dawnward from the inflow direction [*Russell et al.*, 1981]; we did not account for this effect since the precise position of the stagnation point is not of critical importance in the present study. Figure 10 plots the magnetosheath flow V_r/V_{th}^+ as a function of the angular distance α from the stagnation point. We find that a linear least squares approximation to the AMPTE/IRM observations (requiring $V_r = 0$ at the stagnation point) fits the data surprisingly well:

$$V_r/V_{th}^{\mathrm{msh}+} \approx 0.016\,\alpha$$

(with α expressed in degrees). We have also checked the radial flow hypothesis. Figure 11 shows the velocity jump vectors $V_r/V_{th}^{\mathrm{msh}+}$ projected onto the dayside magnetopause surface in GSM coordinates; separate dawnside and duskside views are presented to avoid the visual effect of foreshortening of the velocity vectors far from the noon meridian. The figure confirms that the velocity jump grows with distance from the stagnation point. The flow indeed appears to be radial, with variations that can be ascribed to the changing dipole tilt angle and solar wind fluctuations. Near the nose of the magnetopause the orientation of the velocity jump appears to be more random. This might be a consequence of the variable position of the stagnation point due to the changing inflow direction and of the larger relative error on the velocity jump. We have also checked that the flow on the magnetospheric side is significantly slower than the magnetosheath flow (note that we consider the velocity jump across the entire MP/LLBL layer, so that convection in the LLBL does not play a role); Figure 11 can therefore be taken to represent the (dimensionless) magnetosheath velocity as well.

The above hypotheses on magnetospheric and magnetosheath flow are precisely those used by *De Keyser and Roth* [this issue]. Using the typical shape of the existence domain derived earlier, they plot the regions on the magnetopause surface (shaded regions in Figures 12b–12f) where TD equilibrium is allowed for magnetic field rotation angles of +180°, +90°, 0°, −90°, and −180°. The sketches put the stagnation point 5° dawnward from the subsolar point. The dipole tilt angle was taken to be zero. Note that the plots of Figures 12b–12f do not represent the state of the magnetopause at any given instant, since θ_B varies from point to point on the magnetopause surface.

The plots indicate that both positive and negative rotation sense may occur near the stagnation point and at the duskside. At the dawnside, however, mainly large positive rotations are expected in the northern hemisphere, while large negative rotations dominate the southern hemisphere. No low-shear dawnside TD equilibrium appears to be possible. This picture is more complicated than the wide RD analysis of *Su and Sonnerup* [1968], who predict an exclusively positive rotation sense in the northern hemisphere and a negative sense in the southern hemisphere. This prediction was found to be inconsistent with ISEE 1 and 2 observations [*Berchem and Russell*, 1982]. It is therefore interesting to review the AMPTE/IRM observations in the light of this prediction.

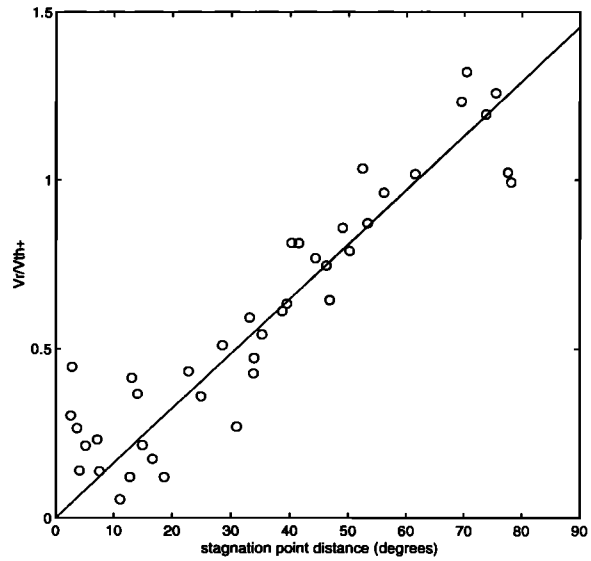

Figure 10. Plot of velocity jump magnitude $V_r/V_{th}^{\mathrm{msh}+}$ as a function of the angular distance α from the stagnation point. The stagnation point position was estimated from the solar wind inflow direction measured right in front of the bow shock. The solid line corresponds to a linear least squares fit.

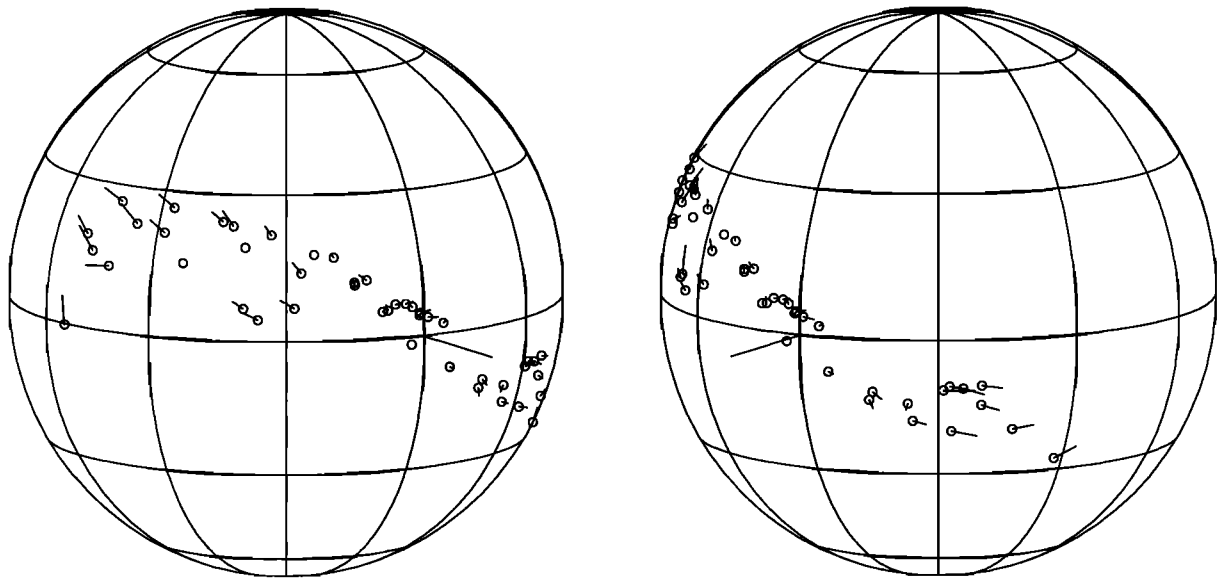

(a) (b)

Figure 11. Views of the velocity jump $V_r/V_{th}^{\mathrm{msh}+}$ across the dayside magnetopause observed during AMPTE/IRM crossings. The subsolar point is indicated by the Earth-Sun line pointing out of the surface. The crossings are indicated by a circle; a line segment indicates the direction of the flow, its length being proportional to the magnitude of the velocity jump. (a) Dawnside (viewed from the 1000 MLT direction). (b) Duskside (viewed from the 1400 MLT direction).

4.2. Observed Sense of Rotation

Figure 13 shows a GSM plot of the magnetic field rotation sense. Crossings are indicated by a plus (positive rotation) or a minus (negative rotation) with a size proportional to the magnitude of the rotation $|\theta_B|$. There are several factors that complicate a direct comparison of this plot with Figure 12:

1. Figure 12 was constructed for zero dipole tilt angle. Changing tilt angle leads to deviations of the magnetospheric field direction at the dawnside and duskside over a range of 32° on either side of the Z^{GSM} axis.

2. Deviations of the mean solar wind inflow direction may shift the location of the stagnation point up to 10° in GSM longitude and latitude. Furthermore, there may be an additional dawnward stagnation point shift depending on the magnetosheath flow [*Russell et al.*, 1981].

3. Solar wind ram pressure variations affect the magnetosheath conditions (both $\boldsymbol{V}^{\mathrm{msh}}$ and $V_{th}^{\mathrm{msh}+}$) and may cause aberrations from the empirical relationship of Figure 10, although the quality of the fit suggests that such deviations tend to be small.

4. The AMPTE/IRM data set contains both TDs and small normal field RDs (see Figure 3). The presence of the latter might obscure the correspondence between predicted and observed existence regions.

As a consequence, the demarcation lines of the regions where TD equilibrium may exist become "fuzzy."

One of the most conspicuous features of Figure 13 is the dominant presence of large positive magnetic field rotations north of the dawnside equator (dawnward of 0900 MLT). *Berchem and Russell* [1982, Figure 2] report on a dawnside crossing in the sourthern hemisphere (0740 MLT, -22° magnetic latitude) with a large ($\approx$ 150°) negative magnetic field rotation. Both findings are in agreement with the DKR model (see Figures 12b and 12f, respectively). Low and high magnetic shear crossings with both positive and negative rotation sense are found to be present near the stagnation point and toward the duskside, consistent with the predictions of the DKR model. Low magnetic shear configurations do not occur dawnward of 0900 MLT, except for the probably nonequilibrium or non-TD low magnetic shear November 10, 1984 crossing (situated at 0812 MLT and 26°N GSM latitude) discussed in the previous section [*Hall et al.*, 1990]. Observations at moderately high northern and southern GSM latitudes near the noon meridian could further substantiate the DKR model. We find that the observed rotation sense generally cannot be explained with the electron whistler polarization theory, a conclusion consistent with the ISEE results [*Berchem and Russell*, 1982].

5. Discussion and Conclusions

This paper was devoted to a study of the magnetic field rotation sense at the dayside magnetopause. In particular, the predictions of the DKR model [*De Keyser and Roth*, 1997a, b, this issue] have been tested with AMPTE/IRM observations.

The first part of this study dealt with the relationship between the magnetic field configuration and the velocity jump across the magnetopause. The purpose of the comparison was to take the observed magnetosheath and magnetospheric states on either side of the magnetopause and to see whether a TD equilibrium would be possible according to the DKR model. The model identifies the ion and electron transition

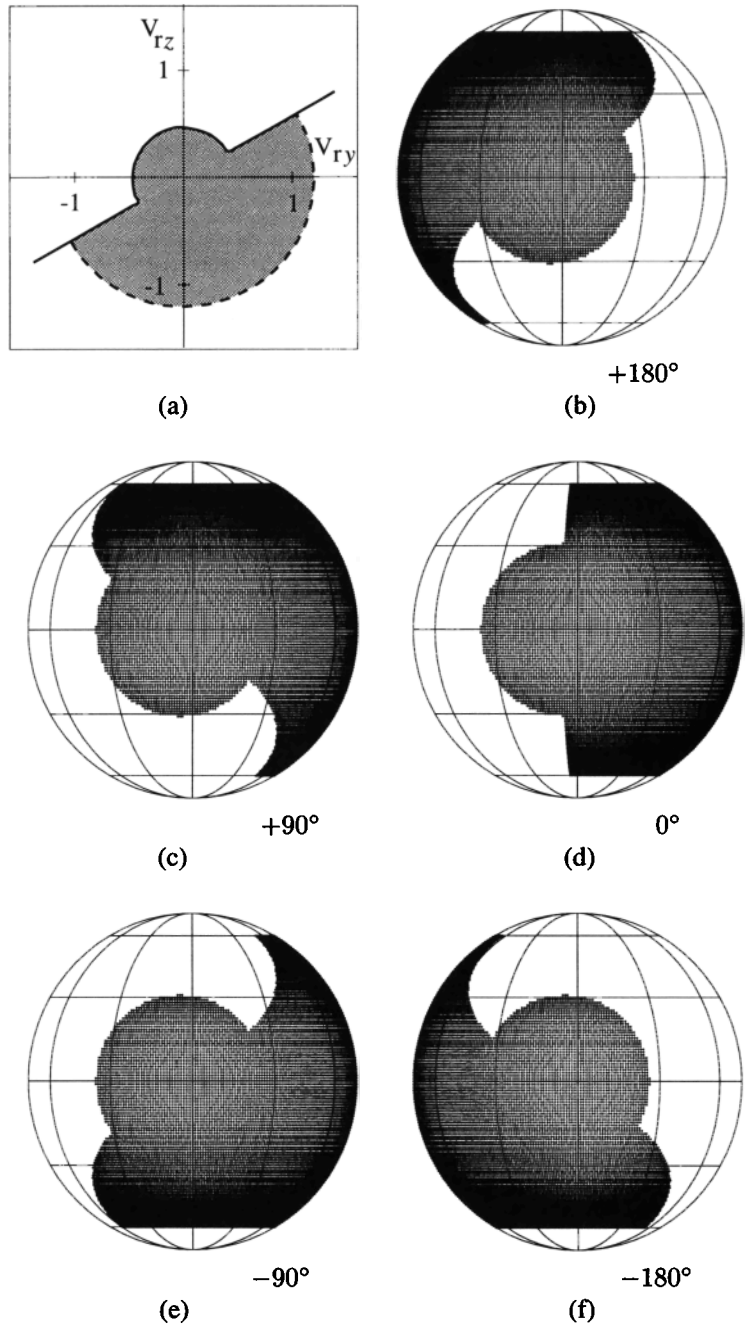

Figure 12. Given a typical velocity jump domain for asymmetric transitions and assuming that the magnetosheath plasma is streaming radially away from the stagnation point according to the empirical relation of Figure 10, it is possible to predict where the dayside magnetopause can be in TD equilibrium for a given magnetic field rotation angle. (a) Sketch of the velocity jump vector domain for a large positive magnetic field rotation. (b) The shaded region indicates where TD equilibrium can exist for a magnetic field rotation angle of +180°, (c) +90°, (d) 0°, (e) −90°, and (f) −180°. The stagnation point is taken to be located 5° dawnward from the subsolar point. The dipole tilt angle is zero. (Figure taken from *De Keyser and Roth* [this issue]).

lengths as the key parameters that control this behaviour. Crude transition length estimates based on thickness approximations support the expectation that $\mathcal{L}_+$ is a few times the ion gyroradius, while $\mathcal{L}_+/\mathcal{L}_-$ is larger than unity but not too large. The good correspondence between the predicted velocity jump vector domain and the TD/RD mix of observations proves that the TDs in the data set obey the DKR existence conditions. Indeed, the only points that seemed not to fit in the predicted picture were the dawnside low-shear crossings whose TD nature had already been questioned in the literature.

In the second part of the paper we applied this result to the configuration at the dayside magnetopause. The observations agree with the predictions of the DKR model regarding

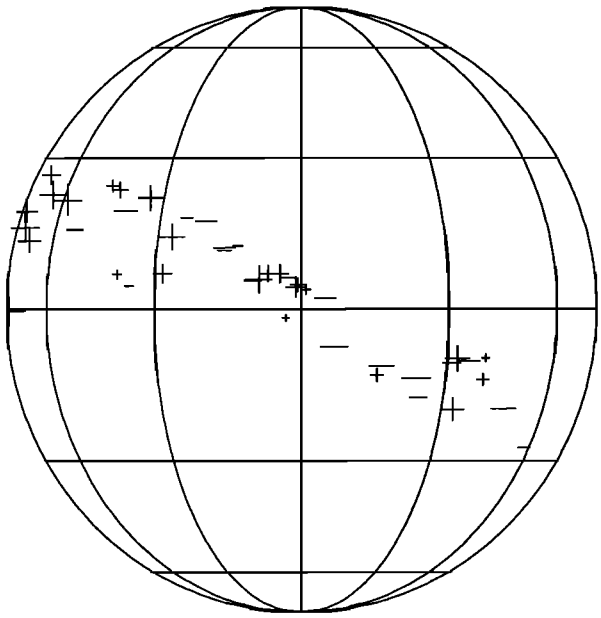

Figure 13. GSM map of magnetopause crossings with the observed magnetic field rotation. A plus indicates a positive (clockwise) rotation; a minus indicates a negative (counterclockwise) rotation sense. The magnitude of the symbol is proportional to the rotation angle. Note the absence of negative rotation sense crossings north of the dawnside equator, and the absence of low-shear dawnside crossings (except for a few cases of questionable TD nature discussed in the text). Near the stagnation point and at the duskside both rotation senses are observed.

(1) the dominant presence of large positive magnetic field rotations north of the dawnside equator, (2) the presence of low and high positive and negative magnetic field rotations near the stagnation point and toward the duskside, and (3) the absence of low magnetic shear TD crossings at the dawnside. Roughly speaking, the situation can be summarized as follows: near the stagnation point both rotation senses are possible; for high magnetic shear ($> 150°$) and far from the stagnation point, the magnetopause is characterized by a positive (clockwise) rotation in the northern hemisphere and a negative (counterclockwise) rotation in the southern hemisphere; for low magnetic shear ($< 60°$) and far from the stagnation point, TD equilibrium appears to be possible only at the duskside.

The fact that the model suggests that the magnetopause really can be a TD everywhere on the dayside is a new and interesting result, something that was not obvious as the effects of velocity shear on the TD magnetopause had not been fully evaluated. This insight may contribute to understanding why, as repeatedly shown by different satellites, the magnetopause sometimes is in a TD state even in configurations where one would expect reconnection to occur, for instance in $\approx 180°$ magnetic shear cases. That high magnetic shear is not a sufficient condition for observing reconnection has been remarked, for instance, by *Paschmann et al.* [1986]. Our result therefore may further the study of the conditions for which reconnection may occur.

A major question raised by the DKR model is: what happens at the low magnetic shear dawnside magnetopause, where TD equilibrium is not possible? Subsolar low-shear transitions have been studied by *Song et al.* [1993], showing a well-defined structure consisting of a "sheath" transition, where the magnetic field change occurs, and a substructured boundary layer. Several low-shear dawnside crossings were analyzed by *Hall et al.* [1990] and *Paschmann et al.* [1990, 1993]. These studies suggest that in such configurations at least part of the LLBL is on open field lines, that is, these transitions probably are not in TD equilibrium. *Mitchell et al.* [1987] conducted an extensive survey of the properties of the LLBL at the magnetospheric flanks and found that the LLBL tends to be thicker with distance from the subsolar point and for northward magnetosheath magnetic field (low magnetic shear). They also observed the dawnside LLBL to be thicker than at the duskside for northward field, but considered the difference not significant. Recent observations by the INTERBALL-Tail probe show unexpectedly large dimensions of the dawnside LLBL, which were noted to occur for northward magnetosheath field [*Sauvaud et al.*, 1997]. These observations are in agreement with the DKR model. They suggest that, as TD equilibrium is lost at the low-shear dawnside magnetopause, plasma can enter the magnetosphere and form an extended LLBL. It is natural to ask what the state of the magnetopause then really is at the dawnside. It might be a rotational discontinuity (this can be difficult to verify observationally, as the MVF is ill defined in low-shear transitions). Perhaps there is no steady state configuration at all; unstable behaviour could be typical for the low-shear dawnside magnetopause. Indeed, high time resolution observations of the ion VDF at the dawnside magnetopause reveal transient behavior in some cases; the lack of information on the magnetic field topology, however, makes it difficult to identify nonstationary reconnection, the Kelvin-Helmholtz instability, or other mechanisms, as the transient process(es) responsible for this behavior [*Vaisberg et al.*, 1997].

The relation between magnetic field configuration and shear flow inferred from the DKR model involves only the plasma conditions on either side of the TD magnetopause. Our test of this relation therefore does not consider structural properties inside the magnetopause. For instance, localized high-speed tangential flows may exist inside the magnetopause. Such high-speed flows have been regarded as the signature of magnetic reconnection [e.g., *Sonnerup et al.*, 1981; *Paschmann et al.*, 1986; *Gosling et al.*, 1990; *Scurry et al.*, 1994; *Phan et al.*, 1996]. We merely wish to note here that the presence of magnetosheath plasma with an enhanced tangential flow speed up to a limited distance earthward of the current layer is also required for tangential discontinuity equilibria. For instance, in the high magnetic shear case, the drift velocity of the inner populations may leave its imprint on the plasma bulk velocity.

Acknowledgments. The authors thank G. Paschmann (Max-Planck-Institut für Extraterrestrische Physik, Garching, Germany) and H. Lühr (Institut für Geophysik und Meteorologie, Technische

Universität, Braunschweig, Germany) for the AMPTE/IRM data. They are also indebted to D. Sibeck (Johns Hopkins University, Applied Physics Laboratory, Laurel, Maryland) for placing the data set on-line and for valuable comments on the manuscript, and to B. T. Tsurutani and J. F. Lemaire for rewarding discussions. The work described in this paper was performed at the Belgian Institute for Space Aeronomy, partly in the framework of the PRODEX/ESA Ulysses Interdisciplinary Study on Directional Discontinuities. The authors acknowledge the support of the Belgian Federal Services for Scientific, Technical and Cultural Affairs.

The Editor thanks Timothy E. Eastman and another referee for their assistance in evaluating this paper.

References

Berchem, J., and C. T. Russell, Magnetic field rotation through the magnetopause: ISEE 1 and 2 observations, *J. Geophys. Res., 87,* 8139–8148, 1982.

Cargill, P. J., and T. E. Eastman, The structure of tangential discontinuities, 1, Results of hybrid simulations, *J. Geophys. Res., 96,* 13,763–13,779, 1991.

De Keyser, J., and M. Roth, Equilibrium conditions for the tangential discontinuity magnetopause, *J. Geophys. Res., 102,* 9513–9530, 1997a.

De Keyser, J., and M. Roth, Correction to "Equilibrium conditions for the tangential discontinuity magnetopause," *J. Geophys. Res., 102,* 19,943, 1997b.

De Keyser, J., and M. Roth, Equilibrium conditions and magnetic field rotation at the tangential discontinuity magnetopause, *J. Geophys. Res.*, this issue.

Eastman, T. E., E. W. Hones, Jr., S. J. Bame, and J. R. Asbridge, The magnetospheric boundary layer: Site of plasma, momentum and energy transfer from the magnetosheath into the magnetosphere, *Geophys. Res. Lett., , 3,* 685–688, 1976.

Eastman, T. E., S. A. Fuselier, and J. T. Gosling, Magnetopause crossings without a boundary layer, *J. Geophys. Res., 101,* 49–57, 1996.

Gosling, J. T., M. F. Thomsen, S. J. Bame, R. C. Elphic, and C. T. Russell, Plasma flow reversals at the dayside magnetopause and the origin of asymmetric polar cap convection, *J. Geophys. Res., 95,* 8073–8084, 1990.

Hall, D. S., M. A. Hapgood, and D. A. Bryant, The transition from the magnetosheath to the magnetosphere, *Geophys. Res. Lett., , 17,* 2039–2042, 1990.

Harris, E. G., On a plasma sheath separating regions of oppositely directed magnetic field, *Nuovo Cimento, 23,* 115–121, 1962.

Kuznetsova, M. M., and M. Roth, Thresholds for magnetic percolation through the magnetopause current layer in asymmetrical magnetic fields, *J. Geophys. Res., 100,* 155–174, 1995.

Kuznetsova, M. M., M. Roth, Z. Wang, and M. Ashour-Abdalla, Effect of the relative flow velocity on the structure and stability of the magnetopause current layer, *J. Geophys. Res., 99,* 4095–4104, 1994.

Lee, L. C., and J. R. Kan, A unified kinetic model of the tangential magnetopause structure, *J. Geophys. Res., 84,* 6417–6426, 1979.

Lühr, H., N. Klöcker, W. Oelschlägel, B. Häusler, and M. Acuna, The IRM fluxgate magnetometer, *IEEE Trans. Geosci. Remote Sens., 23,* 259–261, 1985.

Mitchell, D. G., F. Kutchko, D. J. Williams, T. E. Eastman, L. A. Frank, and C. T. Russell, An extended study of the low-latitude boundary layer on the dawn and dusk flanks of the magnetosphere, *J. Geophys. Res., 92,* 7394–7404, 1987.

Paschmann, G., H. Loidl, P. Obermayer, M. Ertl, R. Laborenz, N. Sckopke, W. Baumjohann, C. W. Carlson, and D. W. Curtis, The plasma instrument for AMPTE/IRM, *IEEE Trans. Geosci. Remote Sens., 23,* 262–266, 1985.

Paschmann, G., I. Papamastorakis, W. Baumjohann, N. Sckopke, C. W. Carlson, B. U. Ö. Sonnerup, and H. Lühr, The magnetopause for large magnetic shear: AMPTE/IRM observations, *J. Geophys. Res., 91,* 11,099–11,119, 1986.

Paschmann, G., B. Sonnerup, I. Papamastorakis, W. Baumjohann, N. Sckopke, and H. Lühr, The magnetopause and boundary layer for small magnetic shear: Convection electric fields and reconnection, *Geophys. Res. Lett., , 17,* 1829–1832, 1990.

Paschmann, G., W. Baumjohann, N. Sckopke, T.-D. Phan, and H. Lühr, Structure of the dayside magnetopause for low magnetic shear, *J. Geophys. Res., 98,* 13,409–13,422, 1993.

Phan, T. D., and G. Paschmann, Low-latitude dayside magnetopause and boundary layer for high magnetic shear, 1, Structure and motion, *J. Geophys. Res., 101,* 7801–7815, 1996.

Phan, T. D., G. Paschmann, and B. U. Ö. Sonnerup, Low-latitude dayside magnetopause and boundary layer for high magnetic shear, 2, Occurrence of magnetic reconnection, *J. Geophys. Res., 101,* 7817–7828, 1996.

Russell, C. T., H.-C. Zhuang, R. J. Walker, and N. U. Crooker, A note on the location of the stagnation point in the magnetosheath flow, *Geophys. Res. Lett., 8,* 984–986, 1981.

Sauvaud, J.-A., P. Koperski, T. Beutier, H. Barthe, C. Aoustin, J. J. Thocaven, J. Rouzaud, E. Penou, O. L. Vaisberg, and N. Borodkova, The INTERBALL-Tail ELECTRON experiment: Initial results on the low-latitude boundary layer of the dawn magnetosphere, *Ann. Geophys., 15,* 587–595, 1997.

Scurry, L., C. T. Russell, and J. T. Gosling, A statistical study of accelerated flow events at the dayside magnetopause, *J. Geophys. Res., 99,* 14,815–14,829, 1994.

Sestero, A., Vlasov equation study of plasma motion across magnetic fields, *Phys. Fluids, 9,* 2006–2013, 1966.

Song, P., C. T. Russell, R. J. Fitzenreiter, J. T. Gosling, M. F. Thomsen, D. G. Mitchell, S. A. Fuselier, G. K. Parks, R. R. Anderson, and D. Hubert, Structure and properties of the subsolar magnetopause for northward interplanetary magnetic field: Multiple-instrument particle observations, *J. Geophys. Res., 98,* 11,319–11,337, 1993.

Sonnerup, B. U. Ö., and L. J. Cahill, Explorer 12 observations of the magnetopause current layer, *J. Geophys. Res., 73,* 1757–1770, 1968.

Sonnerup, B. U. Ö., G. Paschmann, I. Papamastorakis, N. Sckopke, G. Haerendel, S. J. Bame, J. R. Asbridge, J. T. Gosling, and C. T. Russell, Evidence for magnetic field reconnection at the Earth's magnetopause, *J. Geophys. Res., 86,* 10,049–10,067, 1981.

Su, S.-Y., and B. U. Ö. Sonnerup, First-order orbit theory of the rotational discontinuity, *Phys. Fluids, 11,* 851–857, 1968.

Vaisberg, O. L., et al., Initial observations of fine plasma structures at the flank magnetopause with the complex plasma analyzer SCA-1 onboard the Interball Tail Probe, *Ann. Geophys., 15,* 570–586, 1997.

J. De Keyser and M. Roth, Belgian Institute for Space Aeronomy, Ringlaan 3, B-1180 Brussels, Belgium. (e-mail: Johan.DeKeyser@oma.be)

(Received July 10, 1997; revised October 15, 1997;
accepted December 16, 1997.)